

A Bilayer Osteochondral Scaffold with Self-Assembled Monomeric Collagen Type-I, Type-II, and Polymerized Chondroitin Sulfate Promotes Chondrogenic and Osteogenic Differentiation of Mesenchymal Stem Cells

Narjes Rashidi,* Maryam Tamaddon, Chaozong Liu, David D Brand, and Jan Czernuszka

Osteochondral (OC) injuries are suffered by over 40 million patients in Europe alone. Tissue-engineering approaches may provide a more promising alternative over current treatments by potentially eliminating the need for revision surgery and creating a long-term substitute. Herein, the goal is to capture the natural biological and mechanical properties of the joint by developing a bilayer scaffold that is novel in two ways: first, a biomimetic bottom-up approach is used to improve production precision and reduce immunogenicity; monomeric collagen type I and II are self-assembled to fibrils and then processed to 3D scaffolds. Second, to induce a tissue-specific response in mesenchymal stem cells (MSCs), polymerized chondroitin sulfate (PCS) is synthesized and grafted to collagen II and hydroxyapatite (HA) is added to collagen I. Incorporation of PCS into collagen II induces a chondrogenic response by upregulation of COL2A1 and ACAN expression, and incorporation of HA into collagen I stimulates osteogenesis and upregulates the expression of COL1A2 and RUNX2. It is remarkable that MSCs give rise to distinct behavior of chondrogenesis and osteogenesis in the two different regions of the bilayer scaffold. This hybrid scaffold of collagen II-PCS and collagen I-HA offers a great potential treatment for OC injuries.

as osteochondral autologous transplantation and marrow stimulation.^[2–8] Unfortunately, these current techniques lead to the formation of fibrocartilage instead of hyaline cartilage with inferior properties.^[9] Total joint replacement may also require revision surgery within 5–10 years.^[10] Tissue-engineered scaffolds, designed to mimic the natural structure and composition of the joint, could be combined with the patient's own cells to regenerate both cartilage and bone and thus to restore the function of the joint.^[11] However, such a scaffold to provide a long-term solution has not yet been developed. As cartilage and bone require different microenvironments for regeneration, it has been a challenge to develop a highly specialized construct to mimic the structure of osteochondral tissue to support simultaneous regeneration of both tissues. To address this challenge, a bilayer scaffold composed of different materials can be developed to form the

desired tissue on each layer. An example of a scaffold for knee repair is a work by Hu et al., who devised a difunctional regeneration scaffold to improve chondrogenesis and osteogenesis of mesenchymal stem cells in a bilayer structure.^[12]


The majority of bilayer scaffolds to date have been fabricated from synthetic polymers or insoluble naturally fibrillar

1. Introduction

Osteochondral injuries mainly caused by progressive osteoarthritis are a major cause of pain and disability in adults.^[1] Tissue-engineering approaches are expected to provide a more promising alternative to current treatments such

N. Rashidi, J. Czernuszka
Department of Materials
University of Oxford
Parks Road, Oxford OX1 3PH, UK
E-mail: narjes_rashidi@yahoo.com

M. Tamaddon, C. Liu
The Royal National Orthopaedic Hospital
UCL Institute of Orthopaedics and Musculo-Skeletal Science
University College London
London HA7 4LP, UK

 The ORCID identification number(s) for the author(s) of this article can be found under <https://doi.org/10.1002/anbr.202100089>.

D. D. Brand
Tennessee Department of Health
Memphis VA Medical Centre
Memphis TN 38104, UK

© 2021 The Authors. Advanced NanoBiomed Research published by Wiley-VCH GmbH. This is an open access article under the terms of the Creative Commons Attribution License, which permits use, distribution and reproduction in any medium, provided the original work is properly cited.

DOI: 10.1002/anbr.202100089

(polymeric) collagen type I for both chondrogenic and osteogenic layers.^[13–17] As opposed to polymeric collagens, monomeric collagens (atelocollagen) are highly pure and are devoid of telopeptide determinants, which resolve the issue of collagen antigenicity on donor and recipient species.^[18] The use of monomeric collagens also allows for precision design and fabrication using a biomimetic bottom-up approach. Here, collagen can be self-assembled from monomers to form fibrils and then crosslinked to produce fibers, giving control and reproducibility over the production; other molecules can be incorporated in the process to produce unique matrices with designer properties. In this study we show that using this designer bottom-up approach, an integrated bilayer scaffold can be produced, which can induce distinctive stem cell differentiation. We incorporate polymerized high-molecular-weight CS (PCS) into monomeric type-II collagen (top layer) and hydroxyapatite (HA) into monomeric type-I collagen (bottom layer) to create this bilayer scaffold that produces chondrogenic and osteogenic response when seeded with bone marrow mesenchymal stem cells (BMMSCs).

It is known that BMMSCs have the capacity to differentiate to chondrocytes, osteocytes, and osteoblasts.^[19] The composition of the extracellular matrix (ECM) on which stem cells grow is the key in regulating their differentiation.^[20–23] The primary components of native cartilage are collagen type II and chondroitin sulfate (CS).^[24] Monomeric collagen II has been shown to promote chondrogenic differentiation of human bone marrow mesenchymal stem cells (BMMSCs).^[25] CS is a nonimmunogenic polysaccharide that can enhance cell adhesion, migration, and differentiation.^[24,25] The incorporation of CS in scaffolds can induce chondrogenic differentiation of MSCs and the synthesis of cartilage-specific matrix.^[26,27] However, there are limited binding sites by which collagen and CS can be attached (the carboxyl group of CS attaches to the amine group of collagen);^[28,29] therefore, its benefit to date has been limited. To address this problem and to increase the incorporation of CS, we successfully increased its molecular weight 11-fold (polymerized CS (PCS)). This ensures that biologically relevant amounts of CS can be included in the scaffold. To produce a biomimetic bone-like layer, we used reconstituted collagen I and HA, which are respectively the major protein and mineral of natural bone and have been shown to encourage bone growth.^[30–36]

Bilayer scaffolds were fabricated based on the optimum outcomes obtained from the individually fabricated cartilage and bone scaffolds. It is of great importance to implement a fabrication method to acquire a smooth transition between layers and prevent delamination, which could occur because of elastic mismatch between layers. We achieved a soft and stable transition between the layers by the repeated steps of layer addition and freeze-drying technique. The resultant scaffold's microstructure was characterized by scanning electron microscopy (SEM) and BMMSCs proliferation and differentiation behaviors (on the scaffold) were also examined.

Table 1. Composition and structural characteristics of scaffolds: type of collagen (type I and type II), ultrastructure (reconstituted fibrillar), and the quantity of the components. XCol2 was used as a control for characterization and cell experiments.

Scaffold acronym	Collagen type	Collagen to (CS, PCS, [HA]) weight ratio
XCol2	Crosslinked reconstituted fibrillar collagen type II	
XCol2-CS	Crosslinked reconstituted fibrillar collagen type II	1:0.2
XCol2-PCS	Crosslinked reconstituted fibrillar collagen type II	1:0.4
XCol1-HA	Crosslinked reconstituted fibrillar collagen type I	1:2.33
Bilayer	Crosslinked reconstituted fibrillar collagen type II and type I	

2. Results and Discussion

2.1. Scaffold Microstructural Evaluation and Compositional Characteristics

We fabricated three types of chondrogenic scaffolds (XCol2, XCol2-CS, and XCol2-PCS), an osteogenic scaffold (XCol1-HA), and a bilayer scaffold (Table 1). Figure 1 shows the steps of scaffold production. Fourier transform infrared spectroscopy (FTIR) spectra of scaffolds confirmed that the primary structure of collagens was maintained during the scaffold fabrication (see the Supporting Information). SEM (Figure 2) shows an interconnected microstructure of pores with a similar quotient of circularity (Q) for XCol2-CS and XCol2-PCS. Pores were elliptical and are presented here as an isopeimetric quotient of circularity (Q) with major and minor pore diameters (Table 2). The scaffold stiffness, pore size, and shape can affect cellular attachment, morphology, and differentiation.^[37,38] As shown in Table 1, both cartilage/collagen II scaffolds showed higher circularity (more circular pore shapes) compared to the bone/collagen I scaffold. Therefore, they could be beneficial for chondrogenic differentiation as BMMSCs with a more rounded cell shape have upregulated the expression of chondrogenic markers.^[39,40] During the freezing of collagen suspensions, the number of ice nuclei, the ice front velocity, and the force that acts to oppose ice crystal growth affect the pore size and morphology.^[41–43] Thus, variations in the scaffolds' pore size could be explained by the differences in viscosity of the collagen solutions during freezing.^[44] The increase in viscosity going from XCol2-CS, XCol1-HA to XCol2-PCS follows the decrease in pore size (Table 2). In cartilage scaffolds, smaller pore size is preferred as it helps cell precondensation, leading stem cells toward chondrogenesis.^[45] All of the collagen II scaffolds have a porosity of over 98%. XCol2-PCS provides a significantly higher compressive modulus in relation to other chondrogenic scaffolds ($p < 0.05$). It can be said that the higher relative density gives rise to the higher modulus of XCol2-PCS versus XCol2-CS. In the case of osteogenic scaffolds, the presence of HA increased the scaffold relative density compared to chondrogenic scaffolds and thus provided the scaffold with a

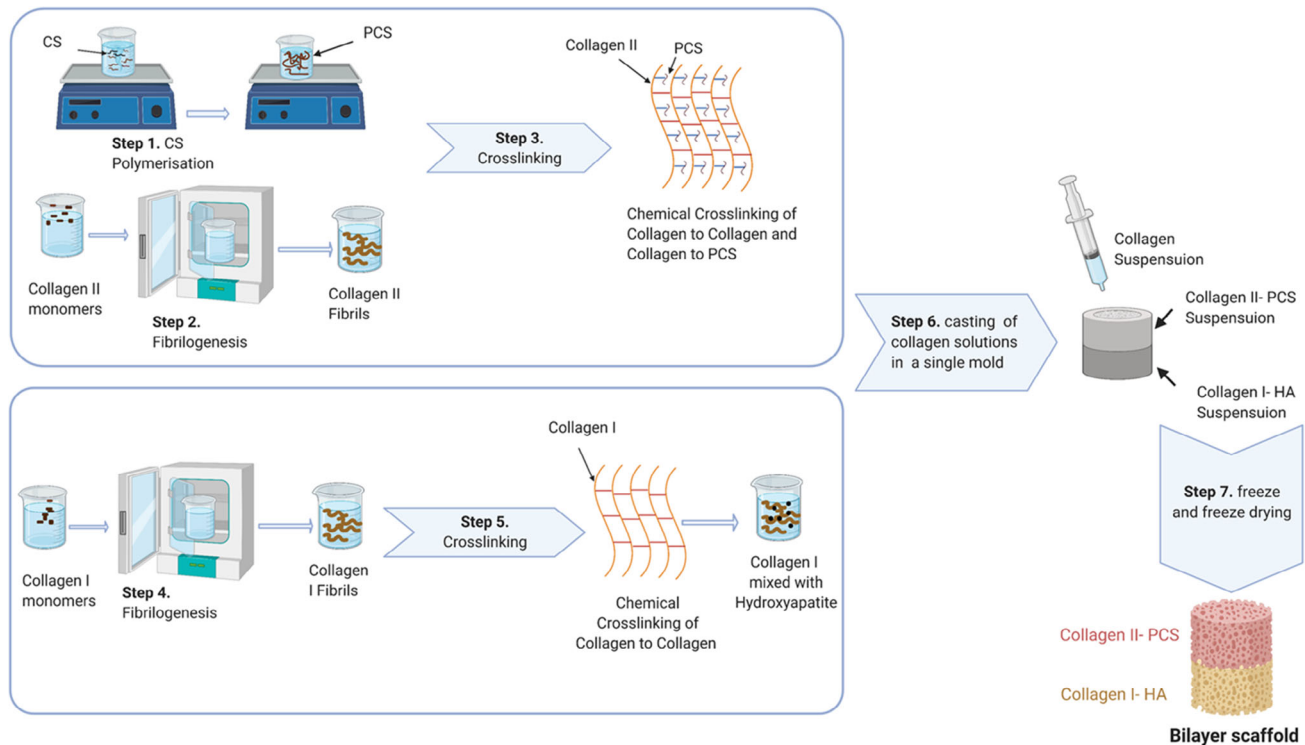


Figure 1. Schematic illustration of the fabrication process of chondrogenic, osteogenic, and bilayer scaffolds.

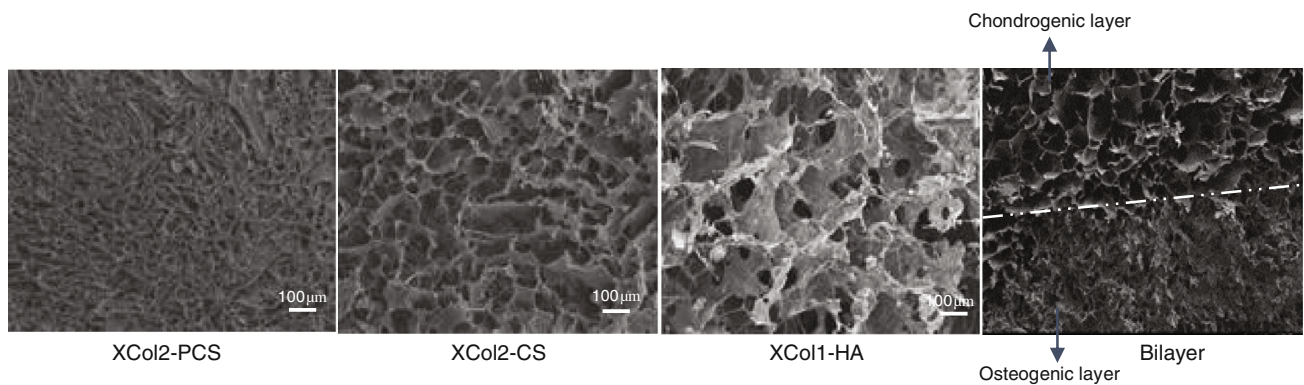


Figure 2. Scaffold microstructure: SEM micrograph showing porous structure of scaffolds; the white dotted line in the bilayer scaffold indicates the interface between the chondrogenic and osteogenic layers.

significantly higher compressive modulus ($p < 0.05$). In this work, the Young's moduli of both chondrogenic and osteogenic scaffolds were increased by one order of magnitude by collagen crosslinking compared to previous work that had only used uncrosslinked collagens.^[44] In addition, crosslinking significantly improved the degradation behavior of scaffolds (see the Supporting Information). To examine CS attachment and release from scaffolds, a total glycosaminoglycan (GAG) assay was performed (Figure 3a,b). More than 80% of the CS incorporated in the uncrosslinked scaffold (Col2-CS) was released into the media in the first hour. The total CS contents of crosslinked scaffolds (XCol2-CS and XCol2-PCS) are approximately seven times

greater than that of the uncrosslinked scaffold and they only released 2% of PCS and 1.2% of CS respectively after 1 h exposure to cell culture media. The CS release was measured for XCol2-CS and XCol2-PCS up to 5 days, where there was insignificant further release over this period. It can thus be concluded that crosslinking gave rise to a large reduction in the CS loss from the scaffolds. Therefore, it is expected that the CS/PCS would remain in the scaffolds for a longer period of time, which would enable them to play their stimulatory role in differentiating stem cells toward the cartilage lineage. The bilayer scaffold was shown to have an integrated interface and relatively smooth transition between the adherent layers (Figure 2). Yet,

Table 2. Structural and mechanical characteristics of scaffolds: compressive moduli ($n=5$) and pore diameters are presented as mean \pm SD; Q = quotient of circularity of pores ($n=100$), η^* = complex viscosity of collagenous suspension at frequency of 0.1 s^{-1} ($n=3$).

Scaffold	Porosity [%]	Major and minor pore diameter [μm]	Relative density (ρ^*/ρ_s)	Compressive modulus [kPa]	Q	η^* [Pa s]
XCol2	98.7	117 \pm 21 60 \pm 11		8.5 \pm 0.8	0.78	
XCol2-CS	98.7	81 \pm 24 43 \pm 13	0.013	28.4 \pm 2.3	0.77	43.4
XCol2-PCS	98.3	61 \pm 14 33 \pm 6.4	0.017	46.4 \pm 7.4	0.78	209
XCol1-HA	97.6	72 \pm 22 40 \pm 12	0.024	71.2 \pm 4.4	0.6	186

differences between cartilage and bone pore morphology and size were still visible.

2.2. PCS Promoted the Cellular Behavior of BMMSCs—Cell Viability, Attachment, and Proliferation

We investigated how sheep BMMSCs adhere, proliferate, and differentiate on the scaffolds up to 21 days (Figure 6a,b). Live/Dead staining at day 21 showed the presence of predominantly viable cells for each scaffold type. Cell colonies can also be seen at day 21 for collagen II scaffolds, which could be associated with pre-cartilage condensation. XCol2-PCS and XCol2-CS scaffolds showed more viable cells at day 21 compared to the XCol1-HA scaffold, indicating a greater proliferation rate (Figure 6b). We support the view that the most reliable strategy for quantifying cell attachment and proliferation in high cell density (100 000 cells/and 3D cultures) is to measure total DNA.^[46] DNA quantification at day 1 as an indication of cell attachment (Figure 3c) demonstrated greater cell attachment for XCol2-PCS over XCol2-CS, which was still greater than XCol2 alone.

Cell proliferation on XCol2-PCS is significantly higher than on XCol2-CS and XCol2 ($p < 0.05$). This shows the beneficial effect of PCS over CS. Collagen II scaffolds showed significantly greater ($p < 0.05$) proliferation rates compared to the XCol1-HA scaffold. The proliferation rates of bilayer scaffolds are higher than that of the XCol1-HA scaffold and lower than those of collagen II scaffolds (Figure 3d).

All the scaffolds irrespective of composition allowed for cell attachment and viability throughout 21 days (Figure 3e). But cells showed significantly different metabolic activity for each composition ($p = 0.003$). Both XCol2-PCS and XCol2-CS showed similar behaviors, and both had increased metabolic activity compared to XCol2 from day 7 onward. XCol1-HA showed a decrease in metabolic activity at day 7, followed by a gradual increase to day 21. For the bilayer scaffold, the metabolic activity decreased at day 7, showing a combined effect of XCol2-PCS and XCol1-HA behaviors, and it was largely unchanged from day 7 onward.

For a cellular solid, the specific surface area ($\frac{SA}{V}$) can be related inversely to the pore diameter (d):^[47] $\frac{SA}{V} \propto \frac{1}{d}$

A lower pore size thus provides potentially a greater surface area for cell ligand binding;^[48] XCol2-PCS has a smaller pore size compared to XCol2-CS, XCol2, and XCol1-HA, giving rise to a higher specific surface area and thus giving rise to greater cell attachment and consequently cell proliferation. Our results in Figure 2 show the relation between cell attachment and pore size. There may be an additional effect of scaffold composition. For example, GAGs have been shown to act as the major ECM adhesion receptors that cooperate in signaling events and effectively regulate the signaling outcomes and proteoglycans promote cell proliferation by acting as growth factor receptors.^[49,50] Accordingly, it can be concluded that, as XCol2-PCS possesses a higher amount of GAGs compared to XCol2-CS and XCol2, it could additionally provide greater cell attachment and proliferation. Coupled with the increase in surface area, XCol2-PCS provides a much more increased effect in cell attachment, as shown (Figure 4).

2.3. PCS-Upregulated Chondrogenic Differentiation of MSCs; Bilayer-Supported Separate Behavior of Chondrogenesis and Osteogenesis in Each Section

Differentiation of MSCs is directed by a network of signaling mechanisms, among which Aggrecan (ACAN) and Runt-related transcription factor 2 (RUNX2) are transcription factors expressed by MSCs upon their differentiation toward chondrogenesis and osteogenesis, respectively.^[51] Expression of Collagen II (COL2A1), Collagen I (COL1A2), Aggrecan (ACAN), and RUNX2 were quantified after 21 days in culture and the results are shown in Figure 5. XCol2-PCS significantly increased the expressions of COL2A1 (10 times) and ACAN (3.2 times) as compared to XCol2-CS (Figure 5a). Therefore, PCS promoted the differentiation of sheep BMMSCs down the chondrogenic lineage over CS. Figure 5b shows that COL1A2 and RUNX2 are expressed for the XCol1-HA scaffold. BMMSCs on the bilayer scaffold showed that each layer gave rise to the expression of different specific markers for each layer (Figure 5c,d). The osteogenic markers expressed significantly higher than chondrogenic markers ($p < 0.05$).

2.4. PCS Increased the Synthesis of Cartilage Matrix; Bilayer Gave Rise to the Formation of Cartilage and Bone Matrix on Each Individual Layer

Alcian Blue staining (Figure 6c) detected a high amount of well-distributed GAGs on XCol2-PCS. The amount of GAGs produced on XCol2-PCS was considerably higher than that produced on XCol2-CS after 21 days. Safranin-O staining (Figure 6d) also represents the formation of abundant cartilage on both collagen II scaffolds. It was shown that XCol2-PCS synthesized significantly a higher amount of cartilage as opposed to XCol2-CS. We have shown that XCol2-PCS increased the formation of the cartilage matrix to a greater extent than XCol2-CS. Although there may be other factors involved, our results show clearly that having additional CS, through polymerization, increases the differentiation of sheep BMMSCs to the chondrogenic lineage with the consequent formation of increased

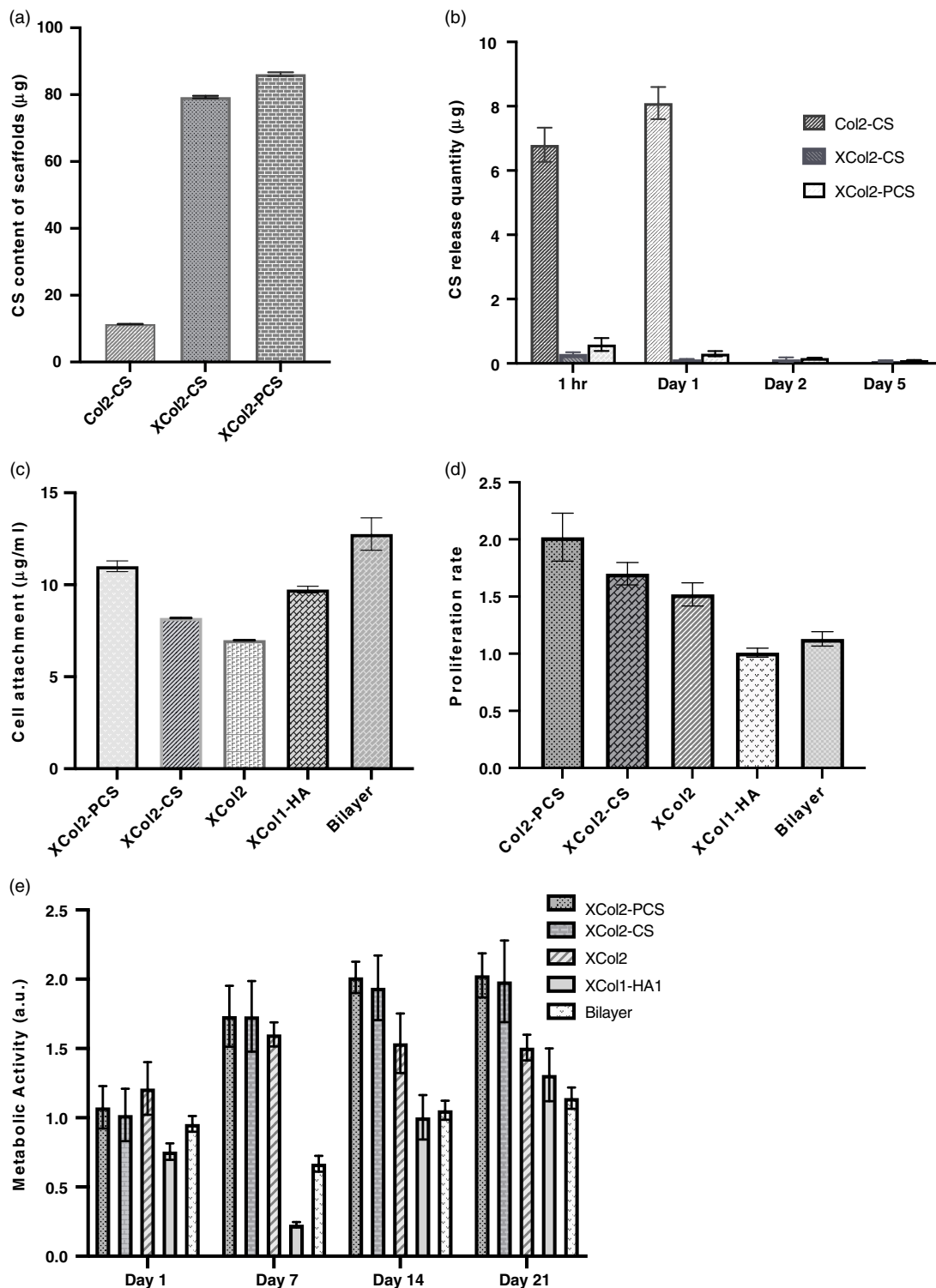


Figure 3. Cell metabolic activity, attachment, and proliferation on the scaffolds: a) initial amount of CS per dry scaffold. b) The amount of CS and PCS released in the cell culture medium during 5 days. c) Cell attachment on chondrogenic, osteogenic, and bilayer scaffolds determined by DNA quantification assay. d) Proliferation rate for chondrogenic scaffolds obtained by the ratio of DNA quantity at day 21 versus day 1. e) Metabolic activity of cells on scaffolds obtained by measuring Presto Blue activity (arbitrary unit: fluorescent intensity). Two-way Analysis of variance (ANOVA) followed by pairwise comparison used to evaluate metabolic activity data, $p < 0.05$.

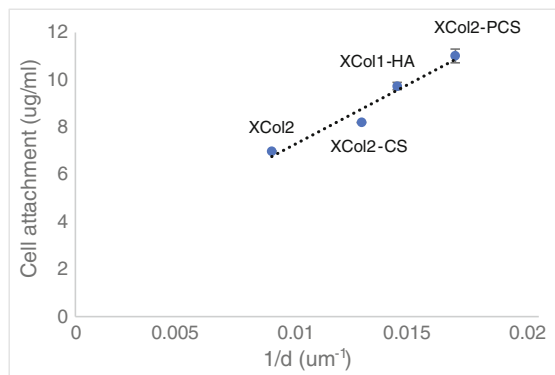


Figure 4. Correlation between a scaffold's cell attachment and specific surface area. Linear regression drives the best fit $y = 517.53x + 2.37$. $R^2 = 0.95$; XCol1-PCS has the greatest surface area (smaller pore size) and accordingly greater cell attachment.

cartilage matrix. XCol1-HA stained positive with Alazarin Red staining indicating calcium-rich deposits (Figure 6c). Figure 6f,g shows that the matrix composition has driven the formation of a cartilage-like matrix and bone-like matrix in separate regions of the bilayer scaffold.

3. Conclusion

To summarize, osteogenic, chondrogenic, and bilayer scaffolds were manufactured from monomeric type-I and type-II collagen. To increase scaffold stability, monomeric collagen solutions were induced to self-assemble and then crosslinked. CS was successfully polymerized to an 11 times higher molecular weight PCS, which was grafted to collagen II. Note that the cell attachment was mainly affected by the specific surface area in chondrogenic (type-II) and osteogenic (type-I) scaffolds, which indicates it was composition-independent. Cellular differentiation and production of ECM markers was affected by the scaffold composition. Collagen type and existence of CS, PCS, and HA affected the type of ECM marker production by cells. It was shown that the presence of PCS stimulated cell differentiation toward chondrogenesis much more than CS. Highly purified collagen II combined with PCS may provide an appropriate microenvironment to promote chondrogenic differentiation and shows superiority over other natural biopolymers. Finally, it was shown that sheep bone marrow mesenchymal stem cells established a separate behavior of chondrogenesis and osteogenesis in the different regions of the bilayer. For future studies, it is recommended that some

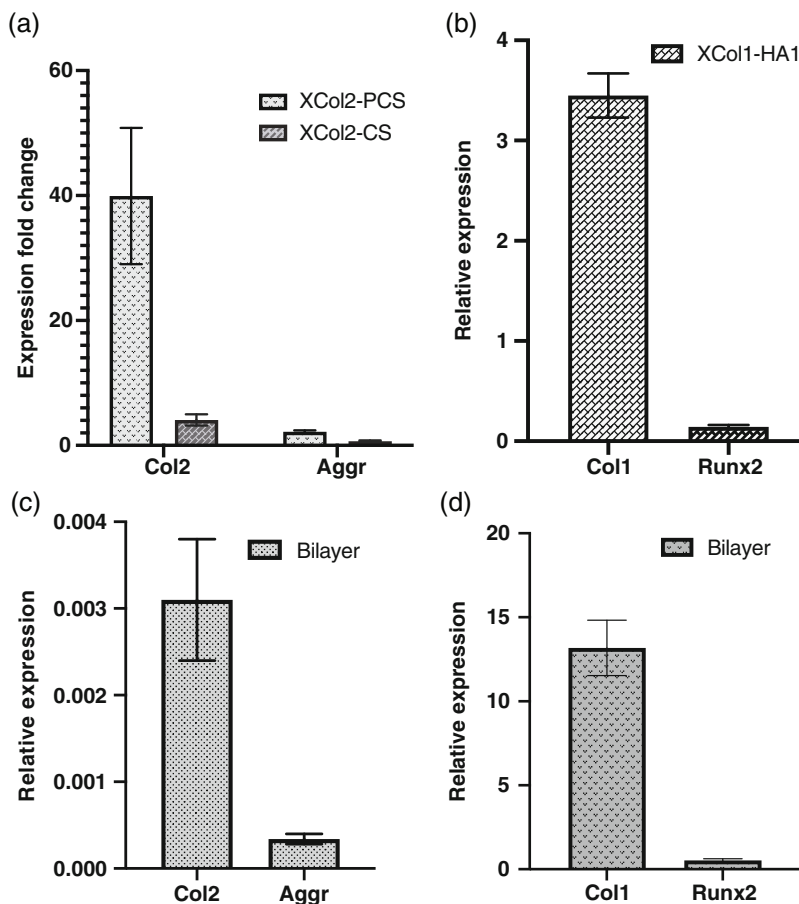


Figure 5. Evaluation of cellular differentiation of sheep BMSCs: a) Collagen II and AGGRECAN expression fold change on XCol2-PCS and XCol2-CS after 21 days (XCol2 scaffolds used as a control). b) Collagen I and RUNX2 relative expression on osteogenic scaffold after 21 days. c,d) Relative expression of chondro- and osteogenic genes on bilayer scaffold. Two-way Anova test was used to assess gene expression data, $p < 0.05$.

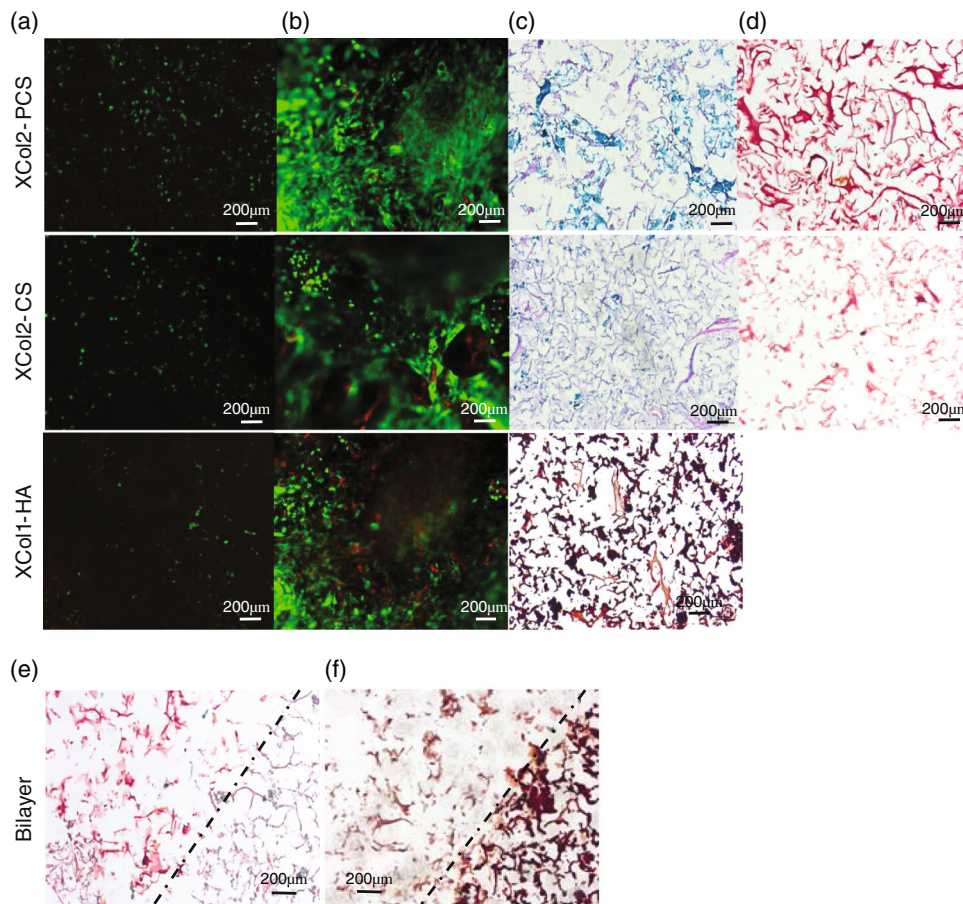


Figure 6. Cell–scaffold interaction and ECM production. a,b) Sheep BMMSC viability by Live/Dead assay on XCol2-PCS, XCol2-CS, and XCol1-HA1 at day 1 and 21; green color indicates live cells and red color indicates dead cells. c,d) Cell matrix production at day 21, Alcian Blue (c) and Safranin-O (d) staining for chondrogenic and Alazarin Red staining for osteogenic scaffolds (c). e,f) Black dotted lines in the bilayer separate the positive staining sections for cartilage and bone ECM.

animal experiments be supplemented to further confirm the in vivo repair ability of this prepared bilayer scaffold.

4. Experimental Section

Scaffold Fabrication: Type-II collagen was extracted from fetal bovine articular cartilage using a limited pepsin digest followed by differential salt fractionation.^[52] Type-I collagen was extracted from fetal bovine skin using a limited pepsin digest followed by differential salt fractionation.^[53,54] Chondroitin sulfate A (from bovine trachea) was purchased from Sigma-Aldrich (Poole, Dorset, UK) and was polymerized based on the modification of a protocol used for crosslinking of polysaccharides.^[55] One percent (w/v) pure fibrillar collagen suspensions (type I and II) were produced by adding lyophilized collagen monomers to dilute acetic acid (pH 3.2). The preparations were then homogenized in an ice bath to reduce the denaturation of collagen. The solutions were then degassed using centrifugation and were induced to self-assemble in tris-buffered saline (TBS) solution in the pH of 7.5 in an incubator at 37 °C for 2 h. Collagen fibrils were crosslinked using 60 mM ethyl-3-(3-dimethylamino-propyl)-carbodiimide (EDC) and 30 mM *N*-hydroxysuccinimide (NHS). Collagen suspensions were injected into the prepared cylindrical polytetrafluoroethylene (PTFE) molds (sealed at one end) and frozen at −20 °C and freeze dried (Christ Alpha 1-5) for 24 h. To produce osteogenic scaffolds, crosslinked reconstituted fibrillar collagen I was prepared. HA was added

to the suspension with the mass ratio of 70% HA to 30% collagen. The suspension was then cast into molds, frozen, and freeze dried. The bilayer scaffold was achieved by the repeated steps of layer addition followed by freeze drying. The thickness of each layer was the same.

Scaffold Characterization: The solution viscosity was measured using an Anton Paar 301 rheometer in oscillatory frequency mode (angular frequency = 0.1–1001 s^{−1}, amplitude = 1%, at 20 °C). To study the microstructure, a Zeiss EVO SEM was operated at the accelerating voltage of 10 kV and probe current of 100 pA and images of different magnifications were taken. The pores were measured using the image processing software ImageJ.

Cell Isolation, Expansion, and Characterization: This study was under the approval of and in compliance with the UK Home Office requirements, Animals (Scientific Procedures) Act 1986, which included local ethical approval by the Royal Veterinary College ethics committee. Bone marrow aspirate was harvested from the iliac crest of adult female sheep under anesthesia using a Jamshidi needle. A 30–50 mL syringe loaded with 1 mL of heparin was used to aspirate the bone marrow up to 20 mL of bone marrow. The aspirate was plated within 6 h of collection in T225 cell culture flasks (ThermoFisher, UK) containing complete media (Dulbecco's Modified Eagles Medium–DMEM, Sigma-Aldrich, UK) supplemented with 10% fetal calf serum (FCS, First Link, UK) and 100 units/mL of penicillin and streptomycin (Gibco, UK) for 3 days under standard conditions (37 °C with 5% CO₂). When cells were 80% confluent, they were passaged. BMMSCs were

characterized by demonstrating their multipotency by differentiating them down the adipogenic, chondrogenic, and osteogenic lineages.

Osteogenic Differentiation: Confluent flasks with sheep BMMSCs at passage 3 were used. 0.5 million cells were seeded into two wells of a 6-well plate (Corning Inc, Corning, USA). The cells were cultured with 1 mL basal medium for 24 h until the culture became fully confluent. Then 1 mL of Stem Pro osteogenic medium (Gibco, Life Technologies, USA) was added to one of the wells and incubated at 37 °C and 5% CO₂ for 21 days. Basal medium was added to the other well to act as a control. The cell culture medium was changed every 3 days. Mineralization was assessed using Alizarin Red stain to identify calcium deposits in the matrix.

Adipogenic Differentiation: The BMMSCs were prepared using the same method described for osteogenic differentiation. However, following the addition of basal media, 1000 µl of adipogenic medium consisting of DMEM supplemented with 10% FCS, 1% PenStrep, 0.5 mM isobutyl-1-methylxanthine, 1 µM dexamethasone, and 10 µg ml⁻¹ insulin were added. Basal medium was added to another well to act as a control. The cells were incubated at 37 °C and 5% CO₂ for 21 days with a medium change every three days. Oil Red O staining was used to identify the lipids in adipocytes.

Chondrogenic Differentiation: For chondrogenic differentiation, 0.5 million cells were suspended in 5 mL of basal medium in two universal tubes and centrifuged in a Heraeus Megafuse centrifuge (ThermoFisher Scientific, USA) at 2000 rpm for 5 min to form a pellet. The universal tubes were placed into an incubator for 24 h to form spheroids. Chondrogenic differentiation medium (Gibco, Life Technologies, USA) was prepared according to the manufacturer's instructions. The basal medium was removed and replaced with 1000 µl of chondrogenic medium and incubated at 37 °C and 5% CO₂ for 21 days. The cell culture medium was changed every 3 days. Alcian Blue staining was used to identify proteoglycans.

In Vitro Cell Seeding: Scaffolds were sterilized by γ irradiation at 25 kGy using a Gammacell 1000 (Best Teratronics Ltd., Hertfordshire, UK), seeded with 2 × 10⁵ sheep BMMSCs, and cultured with chondrogenic medium for the period of 21 days. Osteogenic scaffolds were seeded by 1 × 10⁵ BMMSCs and cultured with osteogenic medium (500 µl in each well). In case of bilayer scaffolds, each layer was seeded by 10⁵ BMMSCs and 800 µl coculture medium (prepared by the mixture of the same volume of chondrogenic and osteogenic scaffolds) was added into each well.

Assessment of Scaffold CS Content and CS Release: To quantify the amount of CS or PCS within scaffolds, scaffolds were digested in a papain solution (2.5 units papain mL⁻¹ in 5 mM cysteine HCl, 5 mM EDTA in phosphate buffered saline, PBS) for 3 h, and sulfated glycosaminoglycan (GAG) content was determined using a Blyscan Kit (Biocolor, UK), as per the manufacturer's instructions. To determine the amount of CS released from scaffolds during the first 5 days of exposure to culture media, media were collected and the CS or PCS content was determined, also per the manufacturer's instructions.

Assessment of Cell Viability, Metabolic Activity, and Cell Proliferation: Sheep BMMSCs' viability on scaffolds was examined by Live/Dead Cell Viability assay (Molecular Probes™, Invitrogen, UK) and was imaged using an ApoTome 2 microscope (Zeiss, Germany). The metabolic activity of cells was investigated using Presto Blue assay (Thermo Fisher scientific, USA) at five time points. Cell proliferation was evaluated using DNA quantification assay. Scaffolds were digested in a papain solution as described earlier and cells were lysed using Cellytic buffer.

Gene Expression Analysis: After 21 days of culturing, total RNA was isolated from the scaffolds using TRIzol reagent (Life technologies, USA). The isolated RNA quality was then verified by a NanoDrop (Spectrophotometer, labtech). cDNA was synthesized from RNA by reverse transcription using Master Mix reagent (Agilliant, USA) and a thermal cycler (Bio-Rad, T100) machine. Gene expression was analyzed by real-time quantitative polymerase chain reaction (qPCR) using a BioRad CFX96 machine. Primer sequences were derived from papers and purchased from Sigma Aldrich.^[56,57] The primer sequences are as follows: b2-microglobulin house-keeping gene (forward: 5-CCAGAAGATGGAAAGCCAAA-3, reverse: reverse: 5-AGCGTGGACAGAAAGGTAG-3), COLII (forward: 5-cctcaagaagctctgtctca-3, reverse: 5-atgtcaatgatgggagacg-3), AGGRECAN (forward: 5-taggtggcgaggaagacatc-3, reverse: 5-aaactgaaaggctctcag-3).

Primers were validated, and their efficiencies were found to be between 0.96 and 1.07. The expression was quantified using the Brilliant III SYBR Green QPCR Master Mix (Agilent, California, USA) kit in accordance with the manufacturer's instructions. The 2^{-ΔCt} method was then used to calculate relative expression of each target gene. Briefly, the mean Ct value of target genes in each sample was normalized to the averaged housekeeping gene Ct value to give a ΔCt value.

Statistical Analysis: ANOVA tests were performed in SPSS for each test. All post hoc tests were Bonferroni corrected for multiple comparisons. Significance was accepted at level of 0.05. If sphericity was violated, Greenhouse Geiser correction values for ANOVA were reported. Experimental groups for each test were as follows—for mechanical testing: n = 5; rheology experiments, metabolic activity, and DNA quantification: n = 3 ; for qPCR test: n = 4.

Supporting Information

Supporting Information is available from the Wiley Online Library or from the author.

Acknowledgements

This work was supported by the Versus Arthritis Research United Kingdom (Grant No. 21977); Innovative United Kingdom via Newton Fund (Grant No. 102872); Engineering and Physical Science Research Council (EPSRC) via DTP case program (Grant No. EP/T517793/1); National Institute for Health Research (NIHR) via NIHR UCLH BRC-UCL Therapeutic Acceleration Support (TAS) Fund (award no: 180340).

Conflict of Interest

The authors declare no conflict of interest.

Data Availability Statement

The data that support the findings of this study are available from the corresponding author upon reasonable request.

Keywords

bilayer osteochondral scaffolds, bone tissue engineering, cartilage tissue engineering, chondroitin sulphate polymerization, collagen scaffolds, mesenchymal stem cells, osteochondral tissue engineering

Received: July 16, 2021

Revised: August 17, 2021

Published online:

- [1] J. A. Buckwalter, H. J. Mankin, *Instr. Course Lect.* **1998**, *47*, 487.
- [2] K. Ronn, N. Reischl, E. Gautier, M. Jacobi, *Arthritis* **2011**, *2011*, 1.
- [3] E. B. Hunziker, *Osteoarthritis Cartilage* **2002**, *10*, 432.
- [4] D. W. Huttmacher, *Biomaterials* **2000**, *21*, 2529.
- [5] E. A. Makris, A. H. Gomoll, K. N. Malizos, J. C. Hu, K. A. Athanasiou, *Nat. Rev. Rheumatol.* **2015**, *11*, 21.
- [6] S. D. McCullen, H. Autebage, A. Callanan, E. Gentleman, M. M. Stevens, *Tissue Eng. Part A* **2012**, *18*, 2073.
- [7] S. P. Nukavarapu, D. L. Dorcemus, *Biotechnol. Adv.* **2013**, *31*, 706.
- [8] J. S. Temenoff, A. G. Mikos, *Biomaterials* **2000**, *21*, 431.
- [9] A. Lynn, R. Brooks, W. Bonfield, N. Rushton, *J. Bone Joint Surgery* **2004**, *86*, 1093.

- [10] G. Labek, M. Thaler, W. Janda, M. Agreiter, B. Stöckl, *J. Bone Joint Surgery* **2011**, 93, 293.
- [11] I. Martin, S. Miot, A. Barbero, M. Jakob, D. Wendt, *J. Biomech.* **2007**, 40, 750.
- [12] X. Hu, Y. Wang, Y. Tan, J. Wang, H. Liu, Y. Wang, S. Yang, M. Shi, S. Zhao, Y. Zhang, Q. Yuan, *Adv. Mater.* **2017**, 29, 1605235.
- [13] S. Zhang, L. Chen, Y. Jiang, Y. Cai, G. Xu, T. Tong, W. Zhang, L. Wang, J. Ji, P. Shi, H. W. Ouyang, *Acta Biomater.* **2013**, 9, 7236.
- [14] P. Giannoni, E. Lazzarini, L. Ceseracciu, A. C. Barone, R. Quarto, S. Scaglione, *J. Tissue Eng. Regenerative Med.* **2015**, 9, 1182.
- [15] J. Zhou, C. Xu, G. Wu, X. Cao, L. Zhang, Z. Zhai, Z. Zheng, X. Chen, Y. Wang, *Acta Biomater.* **2011**, 7, 3999.
- [16] I. Schleicher, K. S. Lips, U. Sommer, I. Schappat, A. P. Martin, G. Szalay, S. Hartmann, R. Schnettler, *J. Surg. Res.* **2013**, 183, 184.
- [17] B. A. Harley, A. K. Lynn, Z. Wissner-Gross, W. Bonfield, I. V. Yannas, L. J. Gibson, *J. Biomed. Mater. Res., Part A* **2010**, 92A, 1066.
- [18] A. K. Lynn, I. V. Yannas, W. Bonfield, *J. Biomed. Mater. Res. Part B: Appl. Biomater.* **2004**, 71B, 343.
- [19] M. F. Pittenger, A. M. Mackay, S. C. Beck, *Science* **1999**, 284, 143.
- [20] S. F. Badylak, *Anatom. Rec. Part B* **2005**, 287B, 36.
- [21] S. Even-Ram, V. Artym, K. M. Yamada, *Cell* **2006**, 126, 645.
- [22] C. M. Murphy, A. Matsiko, M. G. Haugh, J. P. Gleeson, F. J. O'Brien, *J. Mech. Behav. Biomed. Mater.* **2012**, 11, 53.
- [23] G. C. Reilly, A. J. Engler, *J. Biomech.* **2010**, 43, 55.
- [24] J. A. Buckwalter, H. J. Mankin, *J. Bone Joint Surg Am.* **1997**, 79A, 600.
- [25] M. Tamaddon, M. Burrows, S. A. Ferreira, F. Dazzi, J. F. Apperley, A. Bradshaw, D. D. Brand, J. Czernuszka, E. Gentleman, *Sci. Rep.* **2017**, 7, 43519.
- [26] J. L. van Susante, J. Pieper, P. Buma, T. H. van Kuppevelt, H. van Beuningen, P. M. van Der Krann, J. H. Veerkamp, W. B. van den Berg, R. P. H. Veth, *Biomaterials* **2001**, 22, 2359.
- [27] S. Varghese, N. S. Hwang, A. C. Canver, P. Theprungsirikul, D. W. Lin, J. Elisseeff, *Matrix Biol.* **2008**, 27, 12.
- [28] J. Pieper, T. Hafmans, J. Veerkamp, T. Van Kuppevelt, *Biomaterials* **2000**, 21, 581.
- [29] J. Lee, H. Edwards, C. Pereira, S. Samii, *J. Mater. Sci. Mater. Med.* **1996**, 7, 531.
- [30] L. Chen, Z. Wu, Y. Zhou, L. Li, Y. Wang, Z. Wang, Y. Chen, *J. Appl. Polym. Sci.* **2017**, 134, 45271.
- [31] J. Gleeson, N. Plunkett, F. O'Brien, *Eur. Cell Mater.* **2010**, 20, 30.
- [32] M. Kikuchi, S. Itoh, S. Ichinose, K. Shinomiya, J. Tanaka, *Biomaterials* **2001**, 22, 1705.
- [33] L. Ning, H. Malmström, Y. Ren, *J. Oral Implantol.* **2015**, 41, 45.
- [34] X. Ren, V. Tu, D. Bischoff, D. W. Weisgerber, M. S. Lewis, D. T. Yamaguchi, T. A. Miller, B. A. C. Harley, J. C. Lee, *Biomaterials* **2016**, 89, 67.
- [35] M. M. Villa, L. Wang, J. Huang, D. W. Rowe, M. Wei, *J. Biomed. Mater. Res. Part B: Appl. Biomater.* **2015**, 103, 243.
- [36] S. Xu, Z. Qiu, J. Wu, X. Kong, X. Weng, F. Cui, X. Wang, *Tissue Eng. Part A* **2015**, 22, 170.
- [37] H. Chang, Y. Wang, *Regenerative Medicine and Tissue Engineering-Cells and Biomaterials*, Intechopen, Rijeka **2011**.
- [38] A. Matsiko, J. P. Gleeson, F. J. O'Brien, *Tissue Eng. Part A* **2014**, 21, 486.
- [39] S. H. McBride, T. Falls, M. L. Knothe Tate, *Tissue Eng. Part A* **2008**, 14, 1573.
- [40] F. Guilak, D. M. Cohen, B. T. Estes, J. M. Gimble, W. Liedtke, C. S. Chen, *Cell Stem Cell* **2009**, 5, 17.
- [41] M. Azouni, W. Kalita, M. Yemmou, *J. Cryst. Growth* **1990**, 99, 201.
- [42] H. Schoof, L. Bruns, A. Fischer, I. Heschel, G. Rau, *J. Cryst. Growth* **2000**, 209, 122.
- [43] U. G. Wegst, M. Schecter, A. E. Donius, P. M. Hunger, *Philos. Trans. R. Soc. A: Math. Phys. Eng. Sci.* **2010**, 368, 2099.
- [44] M. Tamaddon, R. Walton, D. Brand, J. Czernuszka, *J. Mater. Sci. Mater. Med.* **2013**, 24, 1153.
- [45] A. Di Luca, K. Szlczak, I. Lorenzo-Moldero, *Acta Biomater.* **2016**, 36, 210.
- [46] K. W. Ng, D. T. Leong, D. W. Huttmacher, *Tissue Eng.* **2005**, 11, 182.
- [47] F. J. O'Brien, B. A. Harley, I. V. Yannas, L. J. Gibson, *Biomaterials* **2005**, 26, 433.
- [48] C. M. Murphy, M. G. Haugh, F. J. O'Brien, *Biomaterials* **2010**, 31, 461.
- [49] S. H. Kim, J. Turnbull, S. Guimond, *J. Endocrinol.* **2011**, 209, 139.
- [50] E. Ruoslahti, Y. Yamaguchi, *Cell* **1991**, 64, 867.
- [51] S. G. Almkali, D. K. Agrawal, *Differentiation* **2016**, 92, 41.
- [52] E. F. Rosloniec, M. Cremer, A. H. Kang, L. K. Myers, D. D. Brand, *Curr. Protocols Immunol.* **2010**, 89, 15.5.1.
- [53] A. E. Postlethwaite, W. K. Wong, P. Clements, S. Chatterjee, B. J. Fessler, A. H. Kang, J. Korn, M. Mayes, P. A. Merkel, J. A. Molitor, L. Moreland, N. Rothfield, R. W. Simms, E. A. Smith, R. Speira, V. Steen, K. Warrington, B. White, F. Wigley, D. E. Frust, *Arthritis Rheumatism* **2008**, 58, 1810.
- [54] J. M. Seyer, E. T. Hutcheson, A. H. Kang, *J. Clin. Invest.* **1977**, 59, 241.
- [55] S. Nishimura, *US 6512109B1, Hokkaido Electric Power Co.* **2003**.
- [56] S. Peletto, S. Bertuzzi, C. Campanella, P. Modesto, M. Grazia Maniaci, C. Bellino, D. Ariello, A. Quasso, M. Caramelli, P. L. Acutis, *Int. J. Mol. Sci.* **2011**, 12, 7732.
- [57] C. C. Ude, S. B. Sulaiman, N. M. Hwei, C. H. Cheng, J. Ahmad, N. M. Yahaya, A. B. Saim, R. B. H. Idrus, *PLOS One* **2014**, 9, e98770.